

Climatology of the 10-m wind along the west coast of South American from 30 years of high-resolution reanalysis

David A. Rahn and René D. Garreaud

Departamento de Geofísica, Facultad de Ciencias Físicas y Matemáticas, Universidad de Chile

1. Introduction

Alongshore wind along the west coast of South America is an important component of typical eastern boundary upwelling systems driving offshore Ekman transport near the surface and producing favorable wind stress curl near the shore (Hill et al. 1998). The coastal wind is influenced over various scales from interannual oscillations to the coastal topography and land/sea breezes. While various methods may be used to obtain the wind characteristics (surface meteorology stations at the coast and on buoys, satellite scatterometer measurements, HF radars at the coasts, etc), several issues limit the use of any particular observation and many measurements have limited or inconstant time series in this region. Measurements may be dominated by local features and might not be representative of the larger area. Radiosondes typically have low spatial and temporal resolution. Satellite scatterometer measurements contain a blind spot near the coast and have at most two passes over one area per day.

Observations may be assimilated into a reanalysis to provide the best approximation of the three-dimensional atmospheric state, which is often used for diagnostic studies or as the initialization and boundary conditions for numerical models. Observations are interpolated to a fixed grid and some details are lost, but reanalysis data have several advantages. These include the blending of multiple observations into a single dataset that is physically consistent and regular in space and time. A recent reanalysis project is from the National Center for Environmental Prediction's Climate Forecast System Reanalysis (CFSR, Saha et al. 2010) that has 64 vertical levels and is available at a horizontal resolution of 0.3° with a reanalysis field every six hours and model forecasts every hour since 1979, which is a considerable improvement over older reanalyses at a 2.5° horizontal resolution and 28 vertical levels.

The high-resolution reanalysis shows details of the near-coast 10-m wind and is used here to present the 30-year climatology of the three most prominent low-level wind speed maxima along the western South American coast that occur near Pisco ($14.8^\circ\text{S } 76.6^\circ\text{W}$), Lengua de Vaca (LdV, $30.0^\circ\text{S } 72.2^\circ\text{W}$), and Lavapie ($36.4^\circ\text{S } 73.8^\circ\text{W}$). Note that these points are centered on the

maximum wind speed just offshore (greater wind speed than a nearby coastal surface station and located near the blind spot of the satellite scatterometer).

2. Results

Annual variation of the 10-m wind field is illustrated by a series of two-month averages (Fig. 1). Some assimilation artifacts near the coast are evident. Sharply rising terrain in spectral grids produces noise near abrupt changes due to the Gibb's effect. During austral summer, there are wind maxima near Lavapie and LdV embedded within a broad region of high wind extending over the central Chilean coast (37–25°S). A small wind maximum near Mejillones (23°S) is present during austral winter south of a stagnation zone at the Chile-Peru border, which is present year-round. Off the Peruvian coast, the wind speed is greatest over a broad area centered on Pisco during austral winter. While the mean field is apt at providing a good sense of the spatial distribution, the annual cycle of strong wind events (defined as days when the 00 UTC wind speed is in the upper quartile) at each location is varied (Fig. 2). Pisco and Lavapie have the largest difference between seasons while LdV tends to have strong wind events distributed throughout the year. High wind peaks during July-September in Pisco, October-December in LdV, and January-May in Lavapie. Distributions of the alongshore wind speed (Fig. 3) demonstrate that in Pisco, the variation is normally distributed around the mean that shifts with the annual cycle. During the high wind months at LdV the distribution is close to a normal distribution as well, but during the winter months it becomes skewed towards lower wind events, due to the passage of cyclones leading to a weaker and sometimes reversed (northerly) wind direction. At Lavapie the distribution is skewed toward northerly winds in all seasons, but during the spring and summer months they are clustered around strong southerly wind.

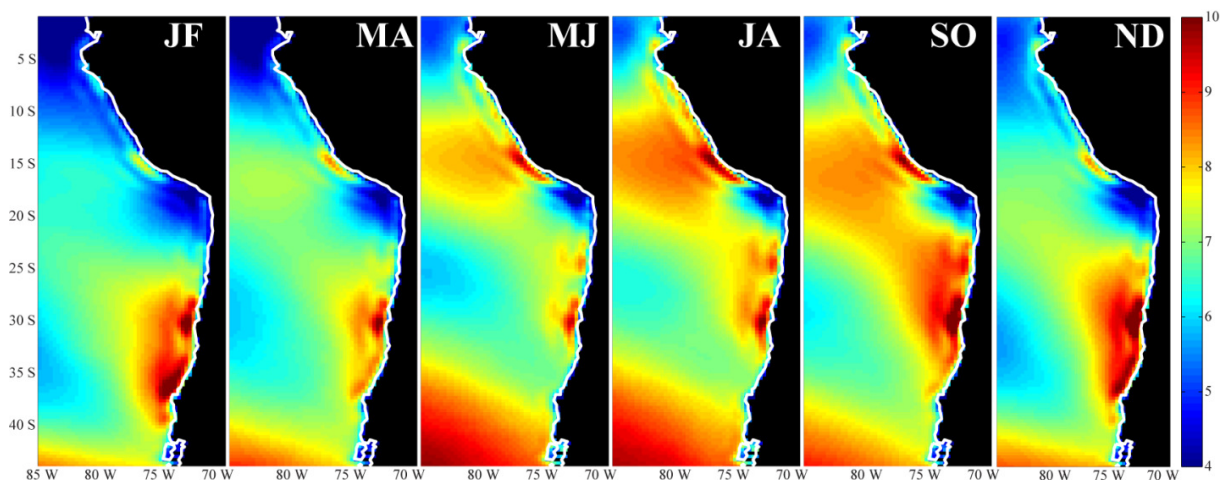


Figure 1. Mean 10-m wind speed (m s^{-1}) at 00 UTC over two-month periods from 1979-2009.

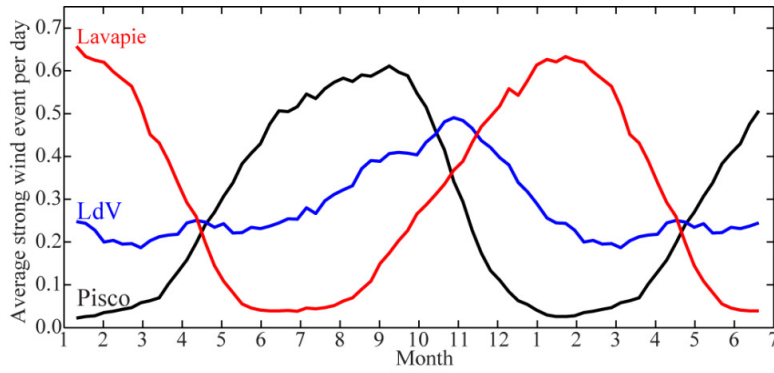


Figure 2. Average strong wind events per day at Pisco (black), LdV (blue), and Lavapie (red).

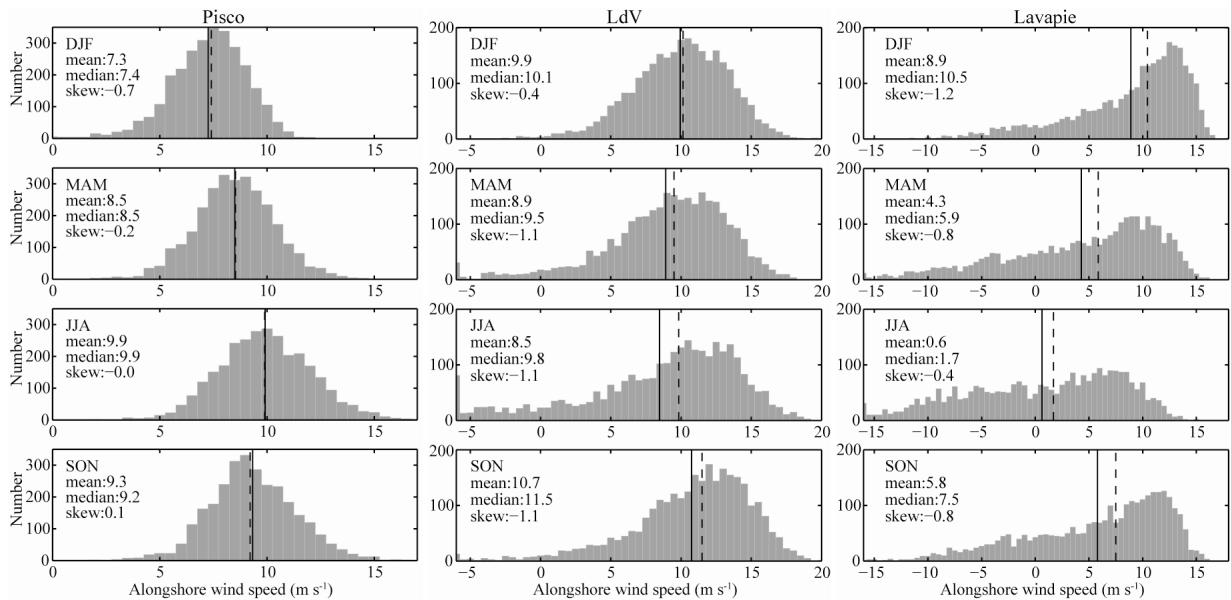


Figure 3. Histogram of the 00 UTC alongshore wind speed (m s^{-1} , positive from the south) for Pisco, LdV, and Lavapie. Months indicated in each panel along with the mean, median, and skewness. Vertical lines represent the mean (solid) and median (dashed).

Composites of high wind days showing anomalies of 10-m wind, surface pressure, and 500-hPa height reveal the differences in the synoptic environments responsible for the high wind at each site. Prior to high wind at Pisco a deep, negatively-tilted trough develops, and prior to high wind at LdV a positively-tilted trough develops but more to the south. Interestingly for Pisco, the surface pressure is anomalously high under the trough, which is due to a much deeper boundary layer (not shown). High wind at Lavapie is associated with ridging and a strengthening of the surface anticyclone. Evolution of the alongshore surface pressure anomaly (Fig. 5) reveals the necessary feature for all three locations is an enhanced alongshore pressure gradient force. For Pisco and LdV, there is a pressure minimum to the south (associated with a cyclone) two

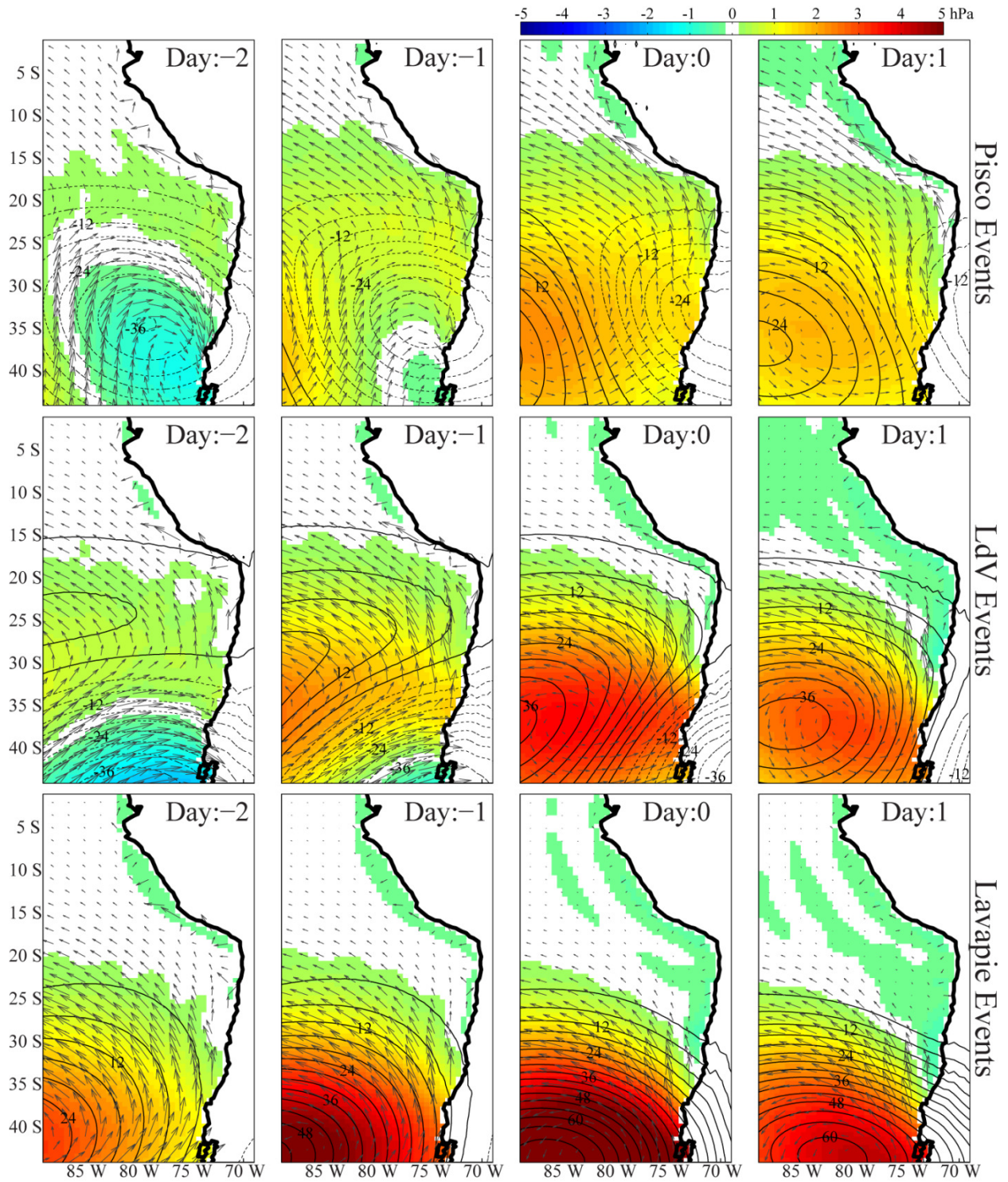


Figure 4. Composites of the 500-hPa height anomalies (m, contours), sea level pressure anomalies (hPa, colors), and 10-m wind anomalies (vectors, m s⁻¹) for (left to right) two days before, one day before, during, and one day after a CJ event at (top) Pisco, (center) LdV, and (bottom) Lavapie.

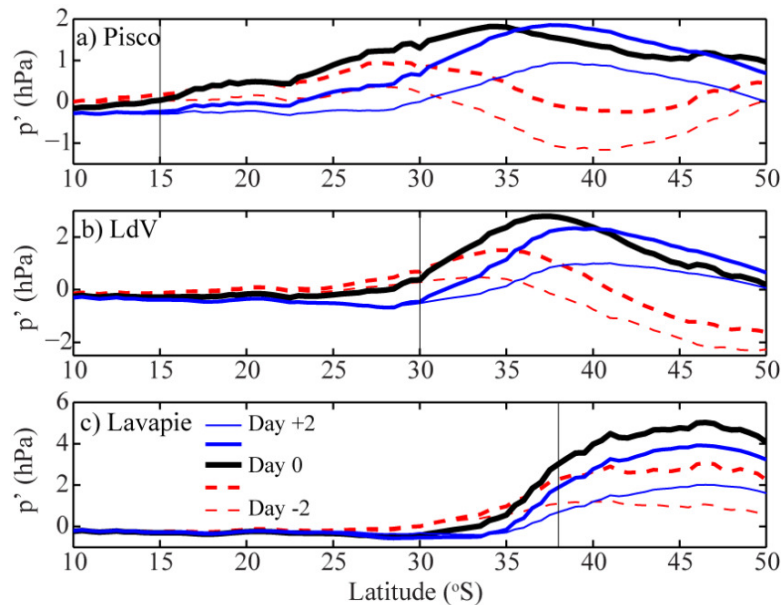


Figure 5. Alongshore pressure perturbations (hPa) associated with strong wind events at (a) Pisco, (b) Ldv, and (c) Lavapie. Day relative to the event is indicated by the key in (c). Location of each station indicated by vertical line.

days prior to the event followed by a positive pressure anomaly. For Pisco there is a broad, extensive anomaly peaking at 35°S, while for Ldv it is concentrated over a much shorter distance. Lavapie is again associated more with a strengthening of the SEP anticyclone than with a migratory feature.

3. Conclusions

With 30 years of high resolution reanalysis data, features of the low-level wind near the coast have been presented including their spatial and temporal distribution. Furthermore, composited synoptic maps highlight the important differences between the synoptic settings that drive the strong wind during each episode. A better representation of the last 30 years of coastal wind along the South America augments our understanding of the current system and may be used as a reference for any future changes to the atmospheric circulation along the coast.

Acknowledgements: This work was supported in part by FONDECYT 3110100.

References

Hill, A. E., B. M. Hickey, F. A. Shillington, P. T. Strub, K. H. Brink, E. D. Barton, and A. C. Thomas, 1998: Eastern ocean boundaries. *The Sea*, A. R. Robinson and K. H. Brink, Eds., The Global Coastal Ocean: Regional Studies and Syntheses, Vol. 11, John Wiley and Sons, 29–67.

Saha, S., and Coauthors, 2010: The NCEP Climate Forecast System Reanalysis. *Bull. Amer. Meteor. Soc.*, **91**, 1015-1057.